ELSEVIER

Computer Methods and Programs in Biomedicine 00 (2003) 1–14

Computer Methods and Programs in Biomedicine

www.elsevier.com/locate/cmpb

Error analysis of a Galerkin method to solve the forward problem in MEG using the boundary element method

Satu Tissari [a,1,*], Jussi Rahola [b,1]

[a] *CSC-Scientific Computing Ltd., P.O. Box 405, 02101 Espoo, Finland*
[b] *Simulintu Oy, Niittykummuntie 6 A 8, 02200 Espoo, Finland*

Received 25 January 2002; received in revised form 4 October 2002; accepted 20 October 2002

Abstract

Sources of brain activity, e.g. epileptic foci, can be localized with Magnetoencephalography (MEG) measurements by recording the magnetic field outside the head. For a successful surgery a very high localization accuracy is needed. The most often used conductor model in the source localization is an analytic sphere, which is not always adequate, and thus a realistically shaped conductor model is needed. In this paper we examine a Galerkin method with linear basis functions to solve the forward problem in MEG using the boundary element method. Its accuracy is compared to the collocation method with constant and linear basis functions. The accuracies are determined for a unit sphere for which analytic solutions are available. The Galerkin method gives a clear improvement in the accuracy of the forward problem especially for the tangential component of the magnetic field. At realistic MEG measurement distances from the brain the Galerkin method reaches a given accuracy with lower computational costs than the collocation methods starting from a few hundreds of unknowns. With larger meshes the difference for the Galerkin method increases significantly.

Keywords: Magnetoencephalography; Boundary element method; Forward problem; Galerkin method; Collocation method

1. Introduction

The sources of brain activity, e.g. epileptic foci, can be localized with Magnetoencephalography (MEG) measurements by recording the magnetic field outside the head [1]. This is called the biomagnetic inverse problem. The localization information can be used in surgical planning. For a successful surgery a very high localization accuracy is needed.

An analytic sphere fitted to the local curvature of the head is the most often used model for the head in the source localization process. The sphere model is not always adequate, e.g. when the source lies deep in the brain, and therefore a realistically shaped conductor model is needed [2]. The surface of the conducting volume is described with a triangular mesh, and the boundary element method (BEM) is used to solve the forward

* Corresponding author. Tel.: +358-9-457-2039; fax: +358-9-457-2302.

E-mail address: satu.tissari@csc.fi (S. Tissari).

[1] The work for this article was mostly carried out in the Parallel Algorithms Project, CERFACS, 42 Av. G. Coriolis, 31057 Toulouse Cedex 01, France.

0169-2607/03/$ - see front matter
doi:10.1016/S0169-2607(02)00144-X

problem, i.e. to calculate the potential and the magnetic field caused by a source in the brain. The source is modeled, e.g. by a point-like electric dipole. The localization process is iterative, where the forward problem has to be usually solved many times. The computed field is compared with the measured field, the source parameters are refined, and the forward problem is computed anew until the desired accuracy is obtained. The accuracy of the forward solution is critical for the localization accuracy.

In this article the accuracy of three methods to solve the forward problem with BEM is studied. The often used collocation method is examined with piecewise constant and linear basis functions. The quality of both these collocation methods used for the calculation of the potential is extensively presented for spheres, ellipses, and cubes by Ferguson and Stroink [3]. Recently, Gençer and Tanzer [4] and Frijns et al. [5] have studied higher-order basis functions with the collocation method on curved geometric elements. The third method is a Galerkin method with piecewise linear basis functions. In addition to the potential we compute also the magnetic field, which can be calculated analytically from the numerically computed potential for both constant [6] and linear [7] basis functions. In the article we provide all the detailed equations needed for the implementation of the methods. The unit sphere with various number of triangular elements is used for the error analysis.

To solve the bioelectromagnetic forward problem the Galerkin method was the first time used by Lynn and Timlake [8] though they called it the triangle mean method. The piecewise linear basis functions with the Galerkin method were for the first time used by Mosher et al. [9], simultaneously with our work [10]. However, the approach of Mosher's paper is different than ours and only the relative error as a function of the dipole depth is dealt with. Our error analysis extends that given in Ref. [9] by studying also the relative error as a function of the number of unknowns and the computational costs involved with different methods. Some interesting phenomena found in the studies are related to mathematical error analyses of the BEM [11].

The bottleneck of the computation of the forward problem is the solution of a large dense system of linear equations. In our article [12], we show how it can be solved by using advanced iterative methods instead of the LU decomposition. In addition, we have combined a precorrected-FFT method with an advanced iterative method to significantly accelerate the solution of the forward problem [13]. Thus, the Galerkin method is used to improve the accuracy of the forward problem and the iterative solver with the precorrected-FFT method is needed to make it possible to use large numbers of unknowns. This method development is necessary for the evaluation of the source localization accuracy of the biomagnetic inverse problem using the BEM with a realistically shaped conductor model [14].

2. Magnetic field and electric potential

2.1. Piecewise homogeneous volume conductor

For a piecewise homogeneous volume conductor consisting of N homogeneous and isotropic parts with associated closed surfaces S_i $(i=1,\ldots,N)$ the magnetic field $\mathbf{B}(\mathbf{r})$ generated by an impressed current and volume currents can be calculated from the Geselowitz's formula [1,15].

$$\mathbf{B}(\mathbf{r}) = \mathbf{B}^{\infty}(\mathbf{r}) + \frac{\mu_0}{4\pi}\sum_{i=1}^{N}(\sigma_i^- - \sigma_i^+) \cdot \int_{S_i} V(\mathbf{r}')\nabla'\left(\frac{1}{|\mathbf{r}-\mathbf{r}'|}\right) \times \mathbf{dS}'. \tag{1}$$

The point $\mathbf{r}$ is outside the conductor, and $\mathbf{dS} = \mathbf{n}\cdot \mathrm{dS}$, where $\mathbf{n}$ is the outward unit normal and dS is the element of area. The conductivities of the regions inside and outside the surface S_i are σ_i^- and σ_i^+, respectively. The potential $V(\mathbf{r})$ has to be computed before obtaining the magnetic field. The infinite medium magnetic field

$$\mathbf{B}^{\infty}(\mathbf{r}) = \frac{\mu_0}{4\pi}\int_G \mathbf{J}_{\mathrm{p}}(\mathbf{r}') \times \frac{\mathbf{r}-\mathbf{r}'}{|\mathbf{r}-\mathbf{r}'|^3}\mathrm{dv}' \tag{2}$$

is generated by the impressed current $\mathbf{J}_{\mathrm{p}}(\mathbf{r})$ as if it were located in an infinite homogeneous volume conductor G of the unit conductivity σ_0.

The potential $V(\mathbf{r})$ can be obtained from the equation [1]

$$(\sigma_r^- + \sigma_r^+)V(\mathbf{r}) = 2\sigma_0 V^\infty(\mathbf{r}) - \frac{1}{2\pi}\sum_{i=1}^{N}(\sigma_i^- - \sigma_i^+)\cdot\int_{S_i} V(\mathbf{r}')\cdot\frac{\mathbf{r}-\mathbf{r}'}{|\mathbf{r}-\mathbf{r}'|^3}\cdot\mathbf{dS}'. \quad (3)$$

The coefficient of the potential inside the integral is the solid angle subtended at $\mathbf{r}$ by the surface element $\mathbf{dS}'$ at $\mathbf{r}'$. The infinite medium potential $V^\infty(\mathbf{r})$ corresponding to the infinite medium magnetic field $\mathbf{B}^\infty(\mathbf{r})$ is:

$$V^\infty(\mathbf{r}) = \frac{1}{4\pi\sigma_0}\int_G \mathbf{J}_\mathrm{p}(\mathbf{r}')\cdot\frac{\mathbf{r}-\mathbf{r}'}{|\mathbf{r}-\mathbf{r}'|^3}\,\mathrm{d}v'. \quad (4)$$

2.2. Method of weighted residuals

An integral equation can be discretized with the method of weighted residuals, where the unknown function is expanded in terms of basis functions on a computational mesh.

In this paper we will concentrate on the homogeneous single-surface model of conductivity σ and surface S, which is sufficient to the MEG [16]. Thus, the integral Eq. (3) for the potential reads

$$V(\mathbf{r}) = \frac{2\sigma_0}{\sigma}\,V^\infty(\mathbf{r}) - \frac{1}{2\pi}\int_S V(\mathbf{r}')\frac{\mathbf{r}-\mathbf{r}'}{|\mathbf{r}-\mathbf{r}'|^3}\cdot\mathbf{dS}'. \quad (5)$$

The potential in Eq. (5) is expressed as the linear combination of M global basis functions $H_i(\mathbf{r})$, $(i = 1,\ldots, M)$:

$$V(\mathbf{r}) = \sum_{i=1}^{M} V_i H_i(\mathbf{r}). \quad (6)$$

The coefficients V_i are the unknown values of the potential. In the method of weighted residuals both sides of the integral equation are multiplied by a weighting function $W_k(\mathbf{r})$ and integrated over the surface of S. We obtain the following linear system for the unknown potential values:

$$\sum_{i=1}^{M} V_i\int_S H_i(\mathbf{r})W_k(\mathbf{r})\mathrm{dS} = 2\frac{\sigma_0}{\sigma}\int_S V^\infty(\mathbf{r})W_k(\mathbf{r})\mathrm{dS} - \frac{1}{2\pi}\sum_{i=1}^{M} V_i\int_S\int_S H_i(\mathbf{r}')\frac{\mathbf{r}-\mathbf{r}'}{|\mathbf{r}-\mathbf{r}'|^3}\cdot\mathbf{dS}'W_k(\mathbf{r})\mathrm{dS}, \quad (7)$$

where $k = 1,\ldots, M$.

The collocation and Galerkin methods can be derived from the above equation using two different kinds of weighting functions [17]. In the collocation method, the weighting functions are delta functions, while in the Galerkin method the weighting functions are the basis functions themselves. The character of the Galerkin method differs from the collocation method in that the Galerkin method tries to satisfy the integral equation everywhere, not only in the collocation points. These discretization methods will be described later in more detail.

The geometry of the homogeneous conductor is described by a triangular mesh. Here, the order of the vertices is assumed to be counterclockwise if looked from outside. The basis functions can be piecewise constant, linear, quadratic, or cubic or even higher orders.

The potential on the surface of the conductor is finally obtained by solving the system of equations. This can be done traditionally by the LU decomposition or by using iterative methods. Because the potential is determined by the integral equations only up to an additive constant, the coefficient matrix is singular. This is removed by adding to each row of the matrix the requirement that the sum of all potential values be zero. The process is called deflation, and it is dealt with in more detail in conjunction with advanced iterative solvers in our second article on the problem [12]. Finally, the magnetic field is calculated from the numerically computed potential.

2.3. Collocation method with constant basis functions

The collocation method is a special case of the method of weighted residuals, where the weighting function is a delta function, $W_k(\mathbf{r}) = \delta(\mathbf{r} - \mathbf{r}_k)$, $k = 1, \ldots, M$. The points $\mathbf{r}_k$ are called the collocation points. This is equivalent to requiring that the original integral equation is satisfied only at the M discrete points on the surface S.

In the collocation method, the basis functions and the collocation points are chosen so that $H_i(\mathbf{r}_k) = 1$, if $i = k$ and 0 otherwise. This leads to a system of equations in the potential $V = (V_1\ V_2\ \ldots\ V_M)^T$:

$$\left(I - \frac{1}{2\pi}\,\Omega\right) V = \frac{2\sigma_0}{\sigma}\ V^{\infty}, \tag{8}$$

where I is the identity matrix. The elements of the square matrix Ω are given by

$$\omega_{ki} = -\int_S H_i(\mathbf{r}')\frac{\mathbf{r}_k - \mathbf{r}'}{|\mathbf{r}_k - \mathbf{r}'|^3} \cdot \mathbf{dS}', \tag{9}$$

and the vector V^{∞} contains the infinite medium potential in all the collocation points.

Here we present the solution procedure, when the piecewise constant basis functions

$$H_i(\mathbf{r}) = \begin{cases} 1 & \mathbf{r} \in \triangle_i \\ 0 & \text{otherwise} \end{cases} \tag{10}$$

are used. The collocation points are the centers of the triangles $\triangle_i$. The potential can be solved from Eq. (8), where the matrix Ω contains the solid angles subtended at the center of each triangle by all other triangles. They can be calculated analytically from [18]

$$\omega_{ki} = 2\arctan\frac{\mathbf{R}_1 \cdot (\mathbf{R}_2 \times \mathbf{R}_3)}{R_1 R_2 R_3 + a + b + c}, \tag{11}$$

where $\mathbf{R}_v = \mathbf{r}_v - \mathbf{r}_k$, $(v = 1, 2, 3)$, $\mathbf{r}_v$ is a vertex of a triangle $\triangle_i$ and $\mathbf{r}_k$ is the center of the observation triangle $\triangle_k$, $R_v = |\mathbf{R}_v|$, $a = R_1(\mathbf{R}_2 \cdot \mathbf{R}_3)$, $b = R_3(\mathbf{R}_1 \cdot \mathbf{R}_2)$, $c = R_2(\mathbf{R}_1 \cdot \mathbf{R}_3)$. The function arctan is computed by a subroutine which gives the result in the correct quadrant.

The magnetic field can be calculated analytically in measurement locations from the potential [6]

$$\mathbf{B}(\mathbf{r}) = \mathbf{B}^{\infty}(\mathbf{r}) + \frac{\mu_0\sigma}{4\pi}\sum_{i=1}^{M} V_i \sum_{k=1}^{3}(\gamma_{k-1}^0 - \gamma_k^0) \cdot (\mathbf{r}_k - \mathbf{r}). \tag{12}$$

where $\mathbf{r}_k$ is the kth vertex of the triangle $\triangle_i$, $\mathbf{r}$ is the measurement location, and

$$\gamma_k^0 = \frac{-1}{|\mathbf{r}_{k+1} - \mathbf{r}_k|} \cdot \ln\frac{|\mathbf{r}_k - \mathbf{r}||\mathbf{r}_{k+1} - \mathbf{r}_k| + (\mathbf{r}_k - \mathbf{r}) \cdot (\mathbf{r}_{k+1} - \mathbf{r}_k)}{|\mathbf{r}_{k+1} - \mathbf{r}||\mathbf{r}_{k+1} - \mathbf{r}_k| + (\mathbf{r}_{k+1} - \mathbf{r}) \cdot (\mathbf{r}_{k+1} - \mathbf{r}_k)}. \tag{13}$$

The infinite medium magnetic field is obtained by Eq. (2).

2.4. Collocation method with linear basis functions

Now we present the collocation method with piecewise linear basis functions. The global linear basis functions $H_i(\mathbf{r})$ are nonzero on all the triangles to which the vertex $\mathbf{r}_i$ belongs. The global linear basis function reaches 1 at the point $\mathbf{r}_i$ and vanishes at the other two vertices of the adjacent triangles. It can be written as a sum of local linear basis functions, that are nonzero only on a single triangle. These are used to simplify the assembly of the coefficient matrices. For each triangle there are three local basis functions, one for each vertex. The local linear basis function $h_i(\mathbf{r})$ for the vertex $\mathbf{r}_i$ of a triangle $\triangle_{kli}$ with vertices $\mathbf{r}_k$, $\mathbf{r}_l$, and $\mathbf{r}_i$ reaches 1, when $\mathbf{r} = \mathbf{r}_i$ and vanishes, when $\mathbf{r} = \mathbf{r}_k$ or $\mathbf{r} = \mathbf{r}_l$:

$$h_i(\mathbf{r}) = \begin{cases} \dfrac{\mathbf{r}_k \cdot \mathbf{r}_l \times \mathbf{r}}{\mathbf{r}_k \cdot \mathbf{r}_l \times \mathbf{r}_i} & \text{if } \mathbf{r} \in \triangle_{kli}. \\ 0 & \text{otherwise} \end{cases} \tag{14}$$

Using the linear basis functions and evaluating Eq. (5) at the collocation points, located at the vertices of the triangles, the potential can be solved from the system of Eq. (8), where the elements of V^{∞} can be obtained by evaluating Eq. (4) in the vertices of the triangles. The matrix Ω is assembled triangle by triangle. The contribution of a single local linear basis function $h_n^t(\mathbf{r})$ of the vertex $\mathbf{r}_n$ of the triangle $\triangle_t$ in the evaluation vertex $\mathbf{r}_i$ is

$$\omega_t^n(\mathbf{r}_i) = -\int_{\triangle_t} h_n^t(\mathbf{r}') \frac{\mathbf{r}_i - \mathbf{r}'}{|\mathbf{r}_i - \mathbf{r}'|^3} \cdot \mathbf{dS}', \tag{15}$$

where the index $n = 1, 2, 3$. These contributions are added to the correct elements of the matrix Ω. The terms ω_t^n can be obtained analytically from Ref. [6]

$$\omega_t^n(\mathbf{r}_i) = 4A_t^{-2}\Bigg(2A_t\Omega_{\triangle_t}(\mathbf{r}_i)(\mathbf{R}_{n+1} \times \mathbf{R}_{n-1}) \cdot \mathbf{n}_t + (\mathbf{R}_1 \cdot \mathbf{R}_2 \times \mathbf{R}_3)(\mathbf{r}_{n+1} - \mathbf{r}_{n-1}) \cdot \sum_{m=1}^{3} (\mathbf{r}_m - \mathbf{r}_{m+1})\gamma_m^0\Bigg), \tag{16}$$

where A_t is the area of triangle $\triangle_t$, $\mathbf{n}_t$ is the unit normal vector of triangle $\triangle_t$, $\Omega_{\triangle_t}(\mathbf{r}_i)$ is the solid angle subtended at the vertex $\mathbf{r}_i$ by the triangle $\triangle_t$ (Eq. (11)), $\mathbf{R}_n$ is $\mathbf{r}_n - \mathbf{r}_i$, and γ_m^0 is given by Eq. (13).

The diagonal elements cannot be calculated by the above equation, because the auto-solid angle $\Omega_{\triangle_t}(\mathbf{r}_i)$ computed for the triangles to which the vertex $\mathbf{r}_i$ belongs is zero, and thus the total solid angle seen by the vertex $\mathbf{r}_i$ is less than 2π. This is often called the auto-solid angle problem. The diagonal elements of the matrix Ω can be obtained by subtracting the sum of other elements on the same row from 2π. When the piecewise constant basis functions are used in the collocation method, there is no auto-solid angle problem, because the solid angles are evaluated in the centers of the triangles, there the total solid angles of the other triangles is always 2π.

For the linear basis functions (Eq. (14)) the magnetic field (Eq. (1)) can be calculated analytically [7]:

$$\mathbf{B}(\mathbf{r}) = \mathbf{B}^{\infty}(\mathbf{r}) + \sum_{i=1}^{M} V_i \mathbf{a}_i(\mathbf{r}), \tag{17}$$

where

$$\mathbf{a}_i(\mathbf{r}) = \frac{\mu_0}{4\pi} \sum_{\triangle_t} \Bigg\{ \sigma \frac{\mathbf{r}_{n+1} - \mathbf{r}_{n+2}}{2A_t} \cdot \Bigg(\sum_{m=1}^{3} \mathbf{n}_t \cdot (\mathbf{c}_m \times \mathbf{c}_{m+1})\gamma_m^0 - (\mathbf{n}_t \cdot \mathbf{c})\Omega_{\triangle_t}(\mathbf{r}) \Bigg) \Bigg\}. \tag{18}$$

The summation over $\triangle_t$ is taken over all the triangles to which the vertex $\mathbf{r}_i$ belongs. The vectors $\mathbf{r}_{n+1}$ and $\mathbf{r}_{n+2}$ are the other two vertices of the triangle $\triangle_t$. The vector $\mathbf{c}$ is a vector from the observation point $\mathbf{r}$ to its perpendicular projection to the plane in which the triangle $\triangle_t$ lies, and $\mathbf{c}_m = \mathbf{r}_m - (\mathbf{r} + \mathbf{c})$. The other symbols are as earlier.

2.5. Galerkin method with linear basis functions

The Galerkin method is a special case of the method of weighted residuals, where the weighting functions $W_k(\mathbf{r})$ are the global basis functions $H_k(\mathbf{r})$. For the Galerkin method Eq. (7) becomes

$$\sum_{i=1}^{M} V_i \int_S H_i(\mathbf{r})H_k(\mathbf{r})\mathrm{dS} = 2\frac{\sigma_0}{\sigma}\int_S V^{\infty}(\mathbf{r})H_k(\mathbf{r})\mathrm{dS} - \frac{1}{2\pi}\sum_{i=1}^{M} V_i \int_S\int_S H_i(\mathbf{r}') \times \frac{\mathbf{r} - \mathbf{r}'}{|\mathbf{r} - \mathbf{r}'|^3} \cdot \mathbf{dS}' H_k(\mathbf{r})\mathrm{dS}. \tag{19}$$

This can be written in matrix notation as

$$(A - B)V = C. \tag{20}$$

where the elements of the matrices A and B and the vector C are given by

$$A_{ki} = \int_S H_i(\mathbf{r})H_k(\mathbf{r})\mathrm{dS}, \tag{21}$$

$$B_{ki} = -\frac{1}{2\pi}\int_S\int_S H_i(\mathbf{r}') \frac{\mathbf{r} - \mathbf{r}'}{|\mathbf{r} - \mathbf{r}'|^3} \cdot \mathbf{dS}' H_k(\mathbf{r})\mathrm{dS}, \tag{22}$$

$$C_i = 2\frac{\sigma_0}{\sigma}\int_S V^{\infty}(\mathbf{r})H_k(\mathbf{r})\mathrm{dS}. \tag{23}$$

Like in the case of the piecewise linear collocation method, the elements of the matrices A and B are assembled triangle by triangle using the local basis functions from Eq. (14). The contribution of each pair of triangles $\triangle_u$ and $\triangle_t$ is added to the correct matrix elements. Each pair of triangles gives rise to a 3×3 matrix, because there are three local basis functions associated with each triangle: $h_{n_u}^u(\mathbf{r})$, $n_u = 1, \ldots, 3$ and $h_{n_t}^t(\mathbf{r})$, $n_t = 1, \ldots, 3$. For the matrix B the 3×3 local contribution is

$$b_{ut}^{n_u n_t} = -\frac{1}{2\pi} \int\int_{\Delta_u \Delta_t} h_{n_t}^t(\mathbf{r}') \frac{\mathbf{r} - \mathbf{r}'}{|\mathbf{r} - \mathbf{r}'|^3} \cdot \mathbf{dS}' h_{n_u}^u(\mathbf{r}) \mathrm{dS}. \quad (24)$$

The inner integral can be computed analytically using Eq. (16). The outer integral is integrated using numerical integration rules for triangles [19]. The local contributions are thus given by

$$b_{ut}^{n_u n_t} = \frac{1}{2\pi} \sum_{j=1}^{P} w_j h_{n_u}^u(\mathbf{r}_j) \omega_t^{n_t}(\mathbf{r}_j). \quad (25)$$

where w_j and $\mathbf{r}_j$ are the weights and abscissae for the P-point integration rule.

There is no auto-solid angle problem in the Galerkin method, because the solid angles are evaluated at the numerical integration points inside the triangles and not at the vertices of the triangles as for the linear collocation method. Like in the case of the constant collocation method, the sum of the solid angles of all the other triangles is 2π.

The matrix A is a sparse matrix whose elements of A_{ki} are nonzero only if the vertices k and i share an edge in the triangular mesh. The contribution from local basis functions is nonzero only if the triangles $\triangle_t$ and $\triangle_u$ are the same. The elements of the matrix A can be computed analytically. The elements of the vector C and the numerical integral in Eq. (25) were computed with 3- and 7-point integration rules. As there was no difference in the results, we used the 3-point rule in the final computations.

The magnetic field is calculated the same way as in the collocation method with the linear basis functions.

2.6. Computational remarks

The number of unknowns is different for various methods when the same triangle mesh is used. In the Galerkin and the linear collocation method the potential is unknown in the vertices of the mesh and in the constant collocation method it is unknown in the center of each triangle. For the same mesh the number of unknowns is about twice for the constant collocation method than for the other methods.

In the Galerkin method the computation of the matrices, especially the matrix B in Eq. (20), is more laborious than in the collocation method. The other computationally intensive step in solving the forward problem is the calculation of the LU decomposition. Its calculation time depends only on the size of the matrix.

3. Results

We will first look at how the computational error behaves for a fixed mesh as a function of the radial coordinate of the source dipole for the various methods. Then we will look at the error versus mesh size, and finally the error versus the computational time for a fixed source dipole.

3.1. Relative error as a function of the radial coordinate of the dipole

The relative error is defined here as

$$\text{relative error} = \sqrt{\sum_i (x_i - \hat{x}_i)^2 / \sum_i x_i^2}, \quad (26)$$

where x_i refers to the analytic solution and $\hat{x}_i$ refers to the numerical one. For the tangential component of the magnetic field the difference in the above equation is replaced by the length of the difference vector. The error in the potential is measured in the integration points of a 13-point integration formula [19] on each triangle of the mesh, and the error in the magnetic field is measured above the integration points, on the spherical surface of radius $1.05R$ where R is the radius of the spherical mesh.

The analytical solutions for the potential and the magnetic field [20,21] are calculated for the unit sphere. The meshes consisting of nearly equilateral triangles are scaled so that the average radius at the numerical integration points is 1.0. The dipole is always tangential.

Because the sum of all unknown potential values is set to zero by deflation in the numerical computation, the same is done for the analytical solution. The analytical potential values computed in the vertices or in the centers of the triangles are averaged to obtain the offset to be subtracted from the samples to be used in the error calculation. The deflation does not effect the magnetic field.

When measuring the relative errors as a function of the radial coordinate of the dipole we used for the constant collocation method a mesh of 2000 triangles and for the other methods a mesh of 4500 triangles. The number of unknowns was 2000 and 2252, respectively. Thus, the methods required roughly the same amount of memory and computer time to solve the linear systems.

3.1.1. Electric potential

The relative error in the potential distribution on the surface of the sphere as a function of the radial coordinate of the dipole is shown in Fig. 1. The Galerkin method gives the best results but the linear collocation method almost reaches the Galerkin method. The constant collocation method loses clearly to the other two methods. However, for all the methods the error increases dramatically and the differences between the methods become smaller when the dipole gets closer to the surface. Also, the improvement in the accuracy gained by increasing the number of the triangles in the mesh weakens clearly towards the surface. However, the accuracy can still be improved by using finer meshes.

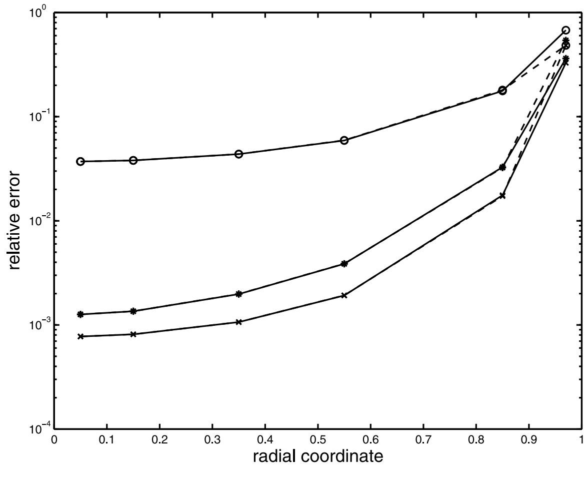

Fig. 1. The relative error in the potential as a function of the radial coordinate of the dipole. The number of unknowns is 2252 for the Galerkin and the linear collocation methods and 2000 for the constant collocation method. The lines with o's, *'s, and x's are for the constant and linear collocation methods, and for the Galerkin method, respectively. The solid and dashed lines are for the dipoles under the center of a triangle and under a vertex, respectively.

The final result, the magnetic field, is computed based on the result of the electric potential. As will be shown in next sections, the relative error of the electric potential and the magnetic field, especially the tangential component of that, behave quite differently.

3.1.2. Tangential component of the magnetic field

The relative error in the tangential component of the magnetic field for all the methods is shown in Fig. 2. Two common observations can be made for all the methods. First, the relative error increases when the dipole moves closer to the origin, because there the magnetic field vanishes. Second, the error increases when the dipole approaches the surface. This shows that the basis functions are too simple to accurately describe the rapid change.

Especially when using a sparse mesh the error curves near the surface are somewhat different for a dipole under a vertex and for a dipole under the center of a triangle. The error of the Galerkin and the linear collocation methods behaves always

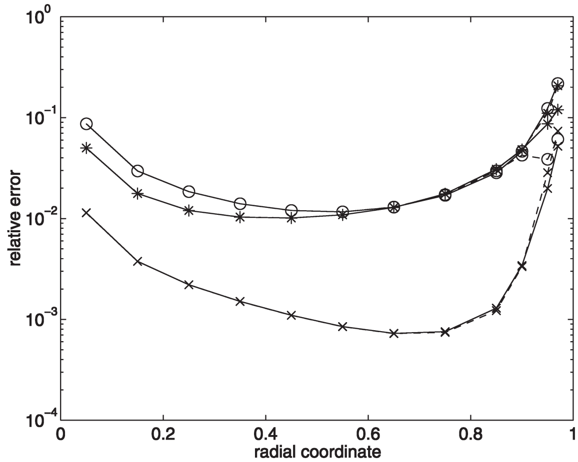

Fig. 2. The relative error in the tangential component of the magnetic field as a function of the radial coordinate of the dipole. The number of unknowns is as in Fig. 1. For line descriptions see the legend of Fig. 1.

smoothly near the surface, and the Galerkin method gives always more accurate results than the linear collocation method. In contrast, the error of the constant collocation method does not increase monotonically when the dipole approaches the surface if the dipole is located under a vertex. However, the overall tendency is the same, i.e. increasing error towards the surface. The constant collocation method reaches the Galerkin method when the dipole is located under a vertex, but is clearly the least accurate if the dipole is located under the center of a triangle.

Generally the constant collocation method gives the least accurate results, but when nodes are added to the mesh the difference between the linear and the constant collocation methods becomes smaller. The Galerkin method gives always clearly the most accurate results.

3.1.3. Radial component of the magnetic field

The relative error in the radial component of the magnetic field as a function of the radial coordinate of the dipole is shown in Fig. 3. The constant collocation method gives clearly the worst results, and there is no significant difference between the linear collocation and Galerkin methods. The surface effect is weak. The differences between the results for a dipole under a vertex and the center of a triangle are clear only very close to the surface. The error in the radial component is almost independent of the dipole radial coordinate except near the origin of the sphere.

For the spherical conductor model the volume currents have no contribution to the radial component of the magnetic field, i.e. the second term of Eq. (1) almost vanishes [1]. The volume currents effect the tangential component of the magnetic field, which has its maximum just above the dipole, where the radial component has its minimum. The biggest errors in the tangential component can be expected to happen near the dipole, because the change in the magnetic field is steepest there. Because the volume currents have no effect on the radial component of the field, its overall error remains also smaller than that of the tangential component and the various discretization methods do not differ essentially from each other. However, this is not valid for realistically shaped conductor models.

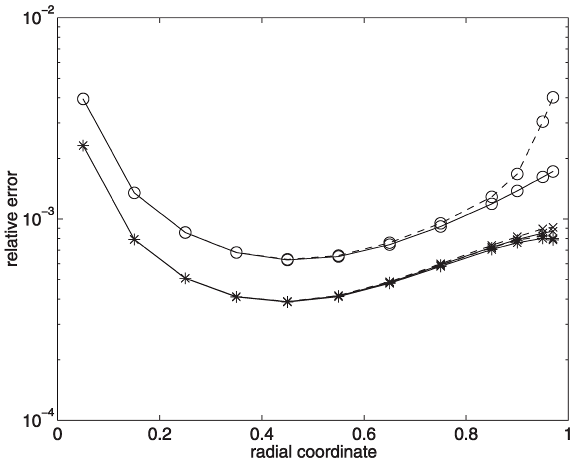

Fig. 3. The relative error in the radial component of the magnetic field as a function of the radial coordinate of the dipole. The number of unknowns is as in Fig. 1. For line descriptions see the legend of Fig. 1.

3.2. Relative error versus the number of unknowns

When measuring the relative errors as a function of the number of unknowns we used meshes with 80–18 000 triangles, i.e. 42–9002 vertices. The

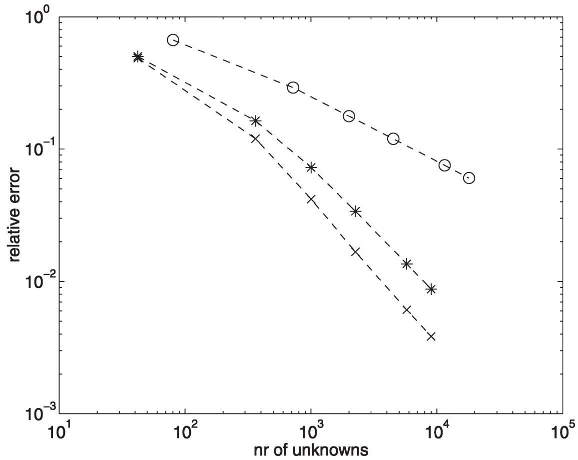

Fig. 4. The relative error in the potential as a function of the number of unknowns. The dashed lines with o's, *'s, and x's are for the constant and linear collocation methods, and the Galerkin method, respectively. Data for Figs. 4–9 is based on the same measurements. Note that both scales are logarithmic.

dipole located under the center of a triangle at the distance of $0.85R$ from the origin of the sphere.

The relative error in the potential as a function of the number of unknowns is shown in Fig. 4. It can be seen that the Galerkin method gives always more accurate results than the collocation methods with the same number of unknowns. However, the difference between the linear collocation method and the Galerkin method is much smaller than the difference between the constant and the linear collocation methods. In addition, as the number of unknowns increases the linear collocation and the Galerkin methods reduce the error approximately with the same rate but with clearly faster rate than the constant collocation method.

The corresponding behaviour of the relative error in the tangential component of the magnetic field is shown in Figs. 5 and 6. The error is measured around the conductor, on the spherical surfaces of radius $1.05R$ (Fig. 5) and $1.3R$ (Fig. 6). The first case is very close to the conductor, and the second case corresponds a realistic MEG recording distance from the brain. Here, we can see that the collocation methods give roughly the same accuracy, and the Galerkin methods gives clearly improved results. In addition, as the number of unknowns increases the accuracy of the Galerkin method initially increases much faster than the accuracy of the collocation methods, and then gradually reaches a significant constant difference to the collocation methods. This observation is more clear when measuring the magnetic field component on the spherical surface of radius $1.3R$ than of radius $1.05R$. In addition,

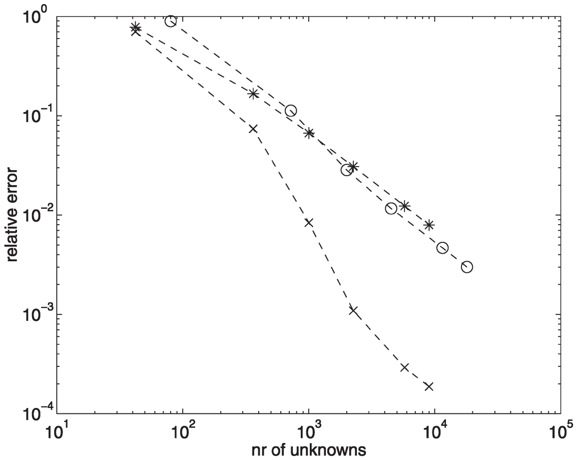

Fig. 5. The relative error in the tangential component of the magnetic field as a function of the number of unknowns. The magnetic field is measured around the conductor on the spherical surface of radius $1.05R$. See the line descriptions in Fig. 4.

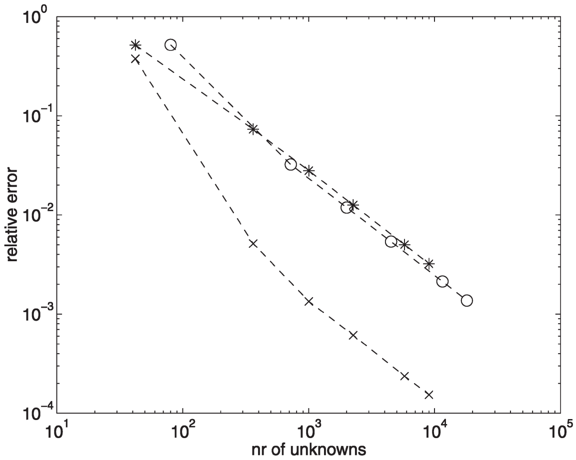

Fig. 6. The relative error in the tangential component of the magnetic field as a function of the number of unknowns. The magnetic field is measured around the conductor on the spherical surface of radius $1.3R$. See the line descriptions in Fig. 4.

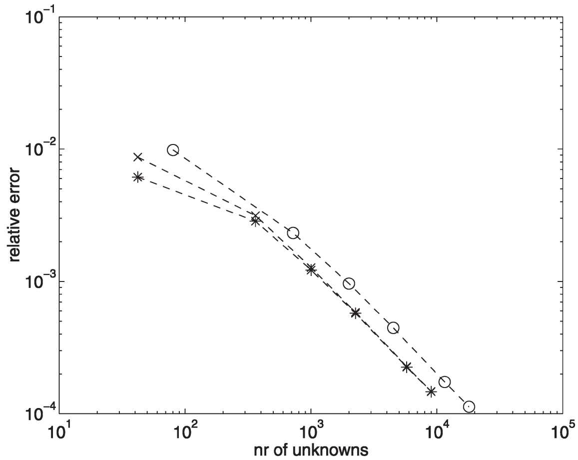

Fig. 7. The relative error in the radial component of the magnetic field as a function of the number of unknowns. The magnetic field is measured around the conductor on the spherical surface of radius $1.3R$. See the line descriptions in Fig. 4.

the difference between the Galerkin method and the collocation methods is significantly greater for a small number of unknowns, e.g. about 400 unknowns, on the spherical surface of radius $1.3R$ than of radius $1.05R$.

The behaviour of the relative error in the radial component of the magnetic field as a function of the number of unknowns is shown in Fig. 7. The errors are measured around the conductor on a spherical surface of radius $1.3R$, and the errors on the spherical surface of radius $1.05R$ are rather similar. The Galerkin method gives the same accuracy as the linear collocation method.

3.3. Relative error versus computational costs

The Galerkin method is more accurate than the collocation methods but more expensive to compute. Here, we study the relative error versus the total computational cost, which is measured by the sum of the time consumed in the assembly of the coefficient matrix and the time taken by the LU decomposition. These are the most laborious steps in solving the forward problem.

In Tables 1–3 we show for all the methods the CPU times for the assembly of the coefficient matrix and for the LU decomposition for several mesh sizes. For the mesh sizes considered here, the matrix assembly of the Galerkin method strongly dominates the LU decomposition. For the linear collocation method these times are comparable, and for the constant collocation method the matrix assembly is negligible compared to the LU decomposition. For still finer meshes the LU decomposition time becomes dominant for all the methods.

All calculations were made on a single R12000 MIPS processor (300 MHz) of a Silicon Graphics Origin using optimization options when compiling the Fortran 90 codes. The LAPACK library [22] was used for the LU decomposition. All the computations were done using double precision arithmetic. There may be variations of about 30% in the measured CPU times due to the varying system load.

The computational costs for the potential are shown in Fig. 8. It can be seen that the Galerkin method is cheaper than the linear collocation method only for large meshes. In addition, there is a significant difference between the constant and linear collocation methods.

Table 1
The CPU times for the assembly of the coefficient matrix T_{mat} and for the LU decomposition T_{LU} for several mesh sizes for the constant collocation method

N_{tri}	N_{un}	T_{mat} (s)	T_{LU} (s)
80	80	6.8E−3	5.7E−3
720	720	0.81	0.49
2000	2000	5.4	11
4500	4500	32	130
11 520	11 520	220	2000
18 000	18 000	510	8000

The mesh size is described by the number of triangles N_{tri} and the number of unknowns N_{un}.

Table 2
The CPU times for the linear collocation method

N_{tri}	N_{un}	T_{mat} (s)	T_{LU} (s)
80	42	2.5E−2	5.9E−4
720	362	1.9	6.5E−2
2000	1002	15	1.4
4500	2252	84	19
11 520	5762	540	260
18 000	9002	1400	990

The mesh size is described by the number of triangles N_{tri} and the number of unknowns N_{un}.

Table 3
The CPU times for the Galerkin method

N_{tri}	N_{un}	T_{mat} (s)	T_{LU} (s)
80	42	0.19	1.9E−2
720	362	16	0.10
2000	1002	120	2.0
4500	2252	630	18
11 520	5762	4300	270
18 000	9002	11 000	1200

The mesh size is described by the number of triangles N_{tri} and the number of unknowns N_{un}.

The corresponding curves for the tangential component of the magnetic field are shown in Fig. 9. It can be clearly seen that the Galerkin method reaches a certain accuracy with less computational time than the other methods when big enough meshes are used. The total computational time with which the Galerkin method becomes more accurate than the collocation methods is shorter when the magnetic field is measured on the spherical surface of radius $1.3R$ than of radius $1.05R$.

From Tables 1–3 we can find out how many unknowns the total computational time of about 16 s corresponds in each method. The number of unknowns is 2000 for the constant collocation method, 1002 for the linear collocation method, and 362 for the Galerkin method. From Fig. 9 it can be seen that for these mesh sizes the Galerkin method gives the smallest relative error. Thus, the Galerkin method is superior to the collocation methods with as less as about 400 unknowns when measuring the magnetic field on the spherical surface of radius $1.3R$. For the larger meshes the difference for the Galerkin method increases even more. This means, that for these mesh sizes the linear collocation method requires about 10 times and the constant collocation method about 40 times as much computer memory as the Galerkin method to obtain a given accuracy in the tangential component of the magnetic field.

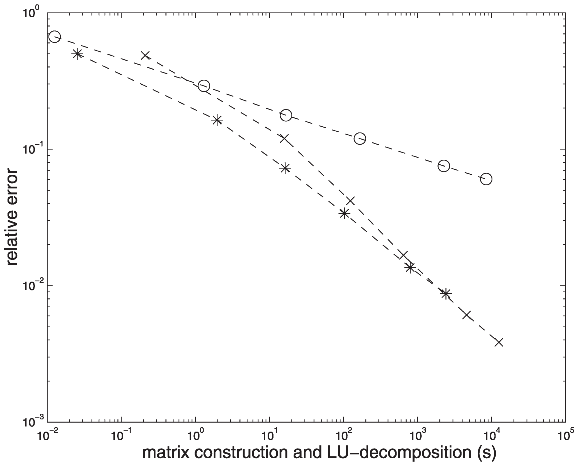

Fig. 8. The relative error in the potential versus the time taken by the assembly of the coefficient matrix and the LU decomposition. The lines with o's, *'s, and x's are for the constant and linear collocation methods, and the Galerkin method, respectively. Note that both scales are logarithmic.

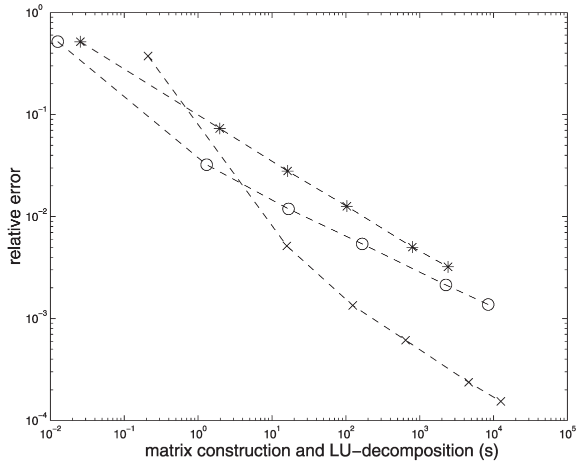

Fig. 9. The relative error in the tangential component of the magnetic field versus the time taken by the assembly of the coefficient matrix and the LU decomposition. For the line descriptions see the legend of Fig. 8.

4. Discussion

We have studied the applicability of a mathematical method called the Galerkin method to the biomagnetic inverse problem. The method is well known and widely used, e.g. in the field of structural analysis. The method is computationally more expensive but more accurate than the other methods used so far. According to our measurements the Galerkin method improves significantly the accuracy of the forward problem especially for the tangential component of the magnetic field. It is shown here to be a competitive alternative to other methods when the number of unknowns is high enough. In practical MEG recording distances from the brain even a small number of unknowns, e.g. 400, is sufficient to make the Galerkin method superior to the collocation methods. Beyond the crossover point, the Galerkin method reaches a desired accuracy clearly more rapidly than the other methods.

The error measurements depend on the choice of measurement points. It is common that the relative error is calculated in the set of points where the unknowns of the numerical approach are to be determined, e.g. in the vertices or the centers of the triangles. Unlike this, we have chosen to measure the error in the 13 integration points on all the triangles. To measure the error only in the collocation points of a given method gives a preference to this method, because the error is minimized in the collocation points. Our choice is fair because the final aim is to obtain a good solution everywhere on the surface of the conductor.

If the unit sphere is discretized so that the vertices of the triangles are on the sphere, the average radius of the tessellated surface is smaller than 1. To increase the compatibility of the analytical unit sphere and the numerical tessellated sphere, we scaled the mesh to have an average radius of 1. This is also needed to facilitate the comparisons between various meshes.

The error for dipoles at an equal distance from the surface varies greatly depending on their location and orientation relative to the vertices [23]. This variation shows that the basis functions are not able to describe the real potential variation on the surface. To give an idea about the variance we have shown the results for dipoles under a vertex and under the center of the triangle with the same orientation. In Ref. [3] 100 dipoles with random locations relative to the vertices were used, and the results were averaged.

It is impossible to directly compare our results for the potential to those presented in other articles because of several differences in the error computation. However, we compared the error values presented in Ref. [3] to ours, and we found that our errors are clearly bigger. The most probable reason for this is that we compute the error for the potential in the integration points instead of the collocation points, where the error is minimized. We also compared our results for the error of the linear Galerkin method to the recent results obtained by Mosher et al. [9], and we found that our results agree qualitatively with those of Mosher.

In Ref. [3] it is reported that the shape of the potential is critical for the localization accuracy, and the numerical solution was scaled by a linear least-squares fit to the analytical one before the error computation. In this process the offset which we subtracted from the analytical solution was also removed. Contrary to the results in Ref. [3] there was only a negligible change in our curves of the relative error versus radial coordinate when the numerical solution was scaled before the error computation. The results presented in this article describe the total error observed in the unscaled data.

The error values for the components of the magnetic field and the potential distribution cannot be directly compared to each other because the scales are different. The potential is determined up to an additive constant, and thus the relative error depends on the offset.

We found that the Galerkin method reduces the error for the tangential component of the magnetic field more rapidly than the linear collocation method when the meshes are refined. This is rather surprising as the errors for the potential are roughly the same for the two methods.

This type of 'superlinear' convergence of the Galerkin method is known in the mathematical error analyses of the BEM [11]. For two-dimensional integral equations similar to the equation described in this paper it can be shown that the error in the Galerkin and collocation methods with piecewise linear basis functions behaves like h^2, where h is the size of the computational element. This estimate is valid when the error is measured in the usual L_2 norm. However, for the Galerkin method it is known that when the error is measured in a negative Sobolev norm $\|\cdot\|_s$, $s = -3$, the error behaves like h^5 [11]. In addition, measuring the error of the magnetic field in the L_2 norm is equivalent to measuring the error of the potential in a negative Sobolev norm [11].

The above discussion gives additional insight into the errors of the Galerkin and collocation methods although we are not aware of rigorous proofs for the current setting. In our three-dimensional case, the number of unknowns N is proportional to h^{-2}, where h is the length of the side of the triangles. The above results would predict convergence rates of N^{-1} for the potential for both methods and for the magnetic field computed using the collocation method. The predicted convergence rate for the magnetic field using the Galerkin method is $N^{-2.5}$. From Figs. 4 and 5 we can estimate the powers k of convergence rate N^k for the potential and the tangential component of the magnetic field. For the linear collocation method we obtain $k = -1.0$ for both the potential and the field, and for the Galerkin method $k = -1.1$ for the potential and $k = -2.3$ for the field in the steepest region, stabilizing to $k = -1.0$ for large meshes.

Acknowledgements

We would like to thank Prof I. Duff for providing S. Tissari with the working facilities in 1998 at CERFACS, where most of the work presented in this article was done. We would also like to thank Prof A. Bendali from CERFACS for providing the triangular meshes of the sphere. More simulations were run later in Finland using the computer system provided by CSC-Scientific Computing Ltd. Finally, we would like to thank the anonymous referees for their constructive comments on the manuscript. Satu Tissari acknowledges the financial support of the Academy of Finland and the Science Foundation of Instrumentarium Corporation, Finland.

References

[1] M. Hämäläinen, R. Hari, R. Ilmoniemi, J. Knuutila, O. Lounasmaa, Magnetoencephalography—theory, instrumentation, and applications to noninvasive studies of the working human brain, Rev. Mod. Phys. 65 (1993) 413–497.

[2] S. Tissari, Realistically shaped conductor model in magnetoencephalography, Licentiate's Thesis, Helsinki University of Technology, Espoo, Finland, 1994.

[3] A.S. Ferguson, G. Stroink, Factors affecting the accuracy of the boundary element method in the forward problem—I: calculating surface potentials, IEEE Trans. Biomed. Eng. 44 (1997) 1139–1155.

[4] N.G. Gençer, I.O. Tanzer, Forward problem solution of electromagnetic source imaging using a new BEM formulation with high-order elements, Phys. Med. Biol. 44 (1999) 2275–2287.

[5] J.H.M. Frijns, S.L. de Snoo, R. Schoonhoven, Improving the accuracy of the boundary element method by the use of second-order interpolation functions, IEEE Trans. Biomed. Eng. 47 (2000) 1336–1346.

[6] J.C. de Munck, A linear discretization of the volume conductor boundary integral equation using analytically integrated elements, IEEE Trans. Biomed. Eng. 39 (1992) 986–990.

[7] A.S. Ferguson, X. Zhang, G. Stroink, A complete linear discretization for calculating the magnetic field using the boundary element method, IEEE Trans. Biomed. Eng. 41 (1994) 455–460.

[8] M.S. Lynn, W.P. Timlake, The use of multiple deflations in the numerical solution of singular systems of equations, with applications to potential theory, SIAM J. Numer. Anal. 5 (1968) 303–322.

[9] J.C. Mosher, R.M. Leahy, P.S. Lewis, EEG and MEG: forward solutions for inverse problems, IEEE Trans. Biomed. Eng. 46 (1999) 245–259.

[10] S. Tissari, J. Rahola, Error analysis of a Galerkin method to solve the forward problem in MEG using the boundary element method, CERFACS Technical Report TR/PA/98/39, CERFACS, 1998.

[11] I.H. Sloan, Error analysis of boundary integral methods, in: Acta Numerica, Cambridge University Press, 1992, pp. 287–339.

[12] J. Rahola, S. Tissari, Iterative solution of dense linear systems arising from the electrostatic integral equation in MEG, Phys. Med. Biol. 17 (2002) 961–975.

[13] S. Tissari, J. Rahola, A precorrected-FFT method to accelerate the solution of the forward problem in MEG, Phys. Med. Biol. 48 (2003) 523–541.

[14] S. Tissari, J. Rahola, J. Nenonen, Source localization accuracy in MEG using the Galerkin method, in: H. Nowak, J. Haueisen, F. Giessler, R. Huonker (Eds.), Proceedings of Biomag 2002, Thirteenth International Conference on Biomagnetism, VDE Verlag, Berlin, 2002, pp. 794–797.

[15] D. Geselowitz, On the magnetic field generated outside an inhomogeneous volume conductor by internal current sources, IEEE Trans. Magn. MAG-6 (1970) 346–347.

[16] M. Hämäläinen, J. Sarvas, Realistic conductivity geometry model of the human head for interpretation of neuromagnetic data, IEEE Trans. Biomed. Eng. 36 (1989) 165–171.

[17] G. Chen, J. Zhou, Boundary Element Methods, Academic Press, London, 1992.

[18] A. van Oosterom, J. Strackee, The solid angle of a plane triangle, IEEE Trans. Biomed. Eng. 30 (1983) 125–126.

[19] K.-J. Bathe, Finite Element Procedures in Engineering Analysis, Prentice-Hall, Englewood Cliffs, NJ, 1982.

[20] D. Yao, Electric potential produced by a dipole in a homogeneous conducting sphere. IEEE Trans. Biomed. Eng. 47 (2000) 964–966/D.A. Brody, F.H. Terry, R.E. Ideker, Eccentric dipole in a spherical medium: generalized expression for surface potentials. IEEE Trans. Biomed. Eng. BME-20 (1973) 141–143.

[21] J. Sarvas, Basic mathematical and electromagnetic concepts of the biomagnetic inverse problem, Phys. Med. Biol. 32 (1987) 11–22.

[22] E. Anderson, Z. Bai, C. Bischof, J. Demmel, J. Dongarra, J.D. Croz, A. Greenbaum, S. Hammarling, A. McKenney, S. Ostrouchov, D. Sorensen, LAPACK Users Guide, SIAM, Philadephia, 1992.

[23] H.A. Schlitt, L. Heller, R. Aaron, E. Best, D.M. Ranken, Evaluation of boundary element methods for the EEG forward problem: effect of linear interpolation, IEEE Trans. Biomed. Eng. 42 (1995) 52–58.